

# Exact diagonalisation study of charge order in the quarter-filled two-leg ladder system $\text{NaV}_2\text{O}_5$

A. Langari<sup>1</sup>, M. A. Martín-Delgado<sup>2</sup> and P. Thalmeier<sup>3</sup>

<sup>1</sup>*Max-Planck-Institute for the Physics of Complex Systems, D-01187 Dresden, Germany*

<sup>2</sup>*Departamento de Física Teórica I, Universidad Complutense, 28040-Madrid, Spain*

<sup>3</sup>*Max-Planck-Institute for Chemical Physics of Solids  
D-01187 Dresden, Germany*

(Feb. 1, 2001)

The charge ordering transition in the layer compound  $\text{NaV}_2\text{O}_5$  is studied by means of exact diagonalization methods for finite systems. The 2-leg ladders of the V-Trellis lattice are associated with one spin variable of the vanadium 3d-electron in the rung and a pseudospin variable that describes its positional degree of freedom. The charge ordering (CO) due to intersite Coulomb interactions is described by an effective Ising-like Hamiltonian for the pseudo-spins that are coupled to the spin fluctuations along the ladder. We employ a Lanczos algorithm on 2D lattice to compute charge (pseudo-spin) and spin-correlation functions and the energies of the low lying excited states. A CO-phase diagram is constructed and the effect of intra-ladder exchange on the CO transition is studied. It is shown that a phase with no-long range order (no-LRO) exists between the in-line and zig-zag ordered structures. We provide a finite-size scaling analysis for the spin excitation gap and also discuss the type of excitations. In addition we studied the effect of bond-alternation of spin exchange and derived a scaling form for the spin gap in terms of the dimerization parameter.

PACS. 71.10.Fd, 75.30.Et, 75.30.Mb

## I. INTRODUCTION

The interplay of charge ordering (CO) and spin structure and dynamics has recently been in the focus of interest especially in the layered 3d-perovskites like cubic and bilayer manganites. A CO transition is caused by inter-site Coulomb interactions dominating the kinetic hopping energy of the electrons of transition elements below a critical temperature  $T_c$ . It localizes the electrons and thus defines an associated low temperature spin lattice which then may exhibit magnetic ordering and possibly low dimensional spin excitations. Such an interplay of charge order and spin excitations, supplemented by a lattice distortion is present in the Trellis lattice compound  $\text{NaV}_2\text{O}_5$ . Its basic building blocks consist of two leg ladders whose rungs are occupied by one d-electron on the average (Fig.1). It is an insulating compound with an effective charge transfer gap given by the hopping  $t_a$  across the rung. The electronic structure of this compound was investigated in Refs. ([1]- [5]) in detail and hopping parameters for a tight binding model were derived. Susceptibility measurements [6] NMR- experiments [7] and x-ray analysis [8] have shown that a spin gap evolves below  $T_c = 33^\circ\text{K}$  at the same time when  $\text{NaV}_2\text{O}_5$  undergoes a CO- transition and lattice distortion. So far there is no complete understanding of both the low temperature structure and the origin of the spin gap.

A model for the coupling of CO to spin degrees of freedom in  $\text{NaV}_2\text{O}_5$  was introduced in Ref. ([9]) based on a pseudospin representation for the rungs such that the

CO transition can be described within a generalized 2D Ising model. Many proposals for the proper low temperature structure have been made. According to the model by Lüdecke et al [8] only every second ladder has zig-zag CO whereas the other ladder stays disordered. This CO is also supported by neutron scattering results [10] discussed in Ref. ([11]). On the other hand, this charge distribution disagrees with an x-ray anomalous scattering measurement which indicates charge modulation along the b-axis [12]. Furthermore the structure in Ref. ([8]) leads to three inequivalent V- sites in valence states  $V^{4+}$ ,  $V^{4.5+}$  and  $V^{5+}$  which is incompatible with NMR results [7] which show that only two inequivalent V-sites exist. A solution of this puzzle has been proposed in Ref. ([13]) where it was shown that this structure actually leads to asymmetric and incomplete charge order where two of the inequivalent sites have almost identical valences. However incomplete charge order complicates the naive application of conventional exchange models for the spin dynamics. Therefore it is first necessary to study the influence of charge ordering on the superexchange mechanism. It was shown [14] how charge correlations in the rungs and CO progressively reduce the superexchange of spins which occupy rung molecular orbitals. For this calculation to be carried through, some mean field like approximations in the charge (pseudo- spin) variables have to be made to start from a restricted orbital space for the calculation of exchange integrals. Finally we mention that some recent results [15] emphasize the fully zig-zag CO in the ladders below  $T_c$  for  $\text{NaV}_2\text{O}_5$ , but the stacking perpendicular to the ladders for this model is still

controversial.

As long as the critical temperature ( $T_c$ ) is finite one may guess that only classical fluctuations are responsible for the phase transition phenomena. However an estimate of the critical point in the whole phase diagram will show whether the quantum fluctuations should be considered. Since the scale of hopping energies and Coulomb interactions are in the order of 1 eV then the critical temperature in this unit is  $T_c=0.0028$  eV. This shows that our model is very close to quantum critical point and quantum fluctuations are very important in the phase transition. Moreover the results at  $T=0$  can explain the phase transition phenomena to a very good extent. It is therefore desirable to do a fully quantum mechanical calculation which treats the charge (pseudo-spin  $\vec{\tau}$ ) and spin  $\vec{\sigma}$  variables of the V-V rungs on the same level. Such an approach is presented in this work and carried through by using exact diagonalisation methods with the Lanczos algorithm. In Sec. II we introduce the pseudospin model that describes the charge ordering transition and the coupling of intra-rung charge fluctuations to the spins. Sec. III is devoted to the description of the numerical methods employed. Sec. IV gives the computational results for the correlation functions and the conjectured phase diagram of CO, furthermore the influence of the spin exchange on the critical CO parameter is studied. In addition we investigate the finite size scaling of the spin excitation gap and its dependence on the degree of charge order. Moreover we have studied the effect of spin exchange bond-alternation on the energy gap and the scaling of spin gap for small value of dimerization  $\gamma$ . A summary of our results is given in Sec. V.

## II. CHARGE ORDERING AND PSEUDO-SPIN MODELS

An attractive feature of the  $\text{NaV}_2\text{O}_5$  compound that simplifies its theoretical study, is the fact that the charge ordering happens to be in an already insulating mixed valent (MV) state. It is characterized by a noninteger valence  $4.5+$  of each vanadium atom of the rung which therefore is occupied by only one d- electron on the average. The ordering is due to the fact that the large intra-rung hopping  $t_a$  leads to a half-filled (rung-) *bonding* band that is separated into an (empty) upper and (filled) lower Hubbard band. The effective insulating gap is then a charge transfer gap approximately given by  $t_a$ . Although this scenario is suggestive, a detailed theory for the insulating state of  $\text{NaV}_2\text{O}_5$  is still lacking. Due to the charge gap, each rung accommodates only one d-electron which can occupy the right (R) or left (L) position of the rung. As first proposed in Ref.( [9]), this charge degree of freedom can be described by an Ising pseudospin variable  $\tau_z$  and its resonating behaviour by the transverse isospin variable  $\tau_x$ . The latter is responsible for the tendency

towards the formation of a bonding state. The Coulomb interactions between d-electrons on different rungs may then be mapped onto Ising-like interactions on the one-particle subspace of the rungs. Altogether the charge degrees of freedom are then described by

$$H_c = -t_a \sum_i \tau_x^i + K \sum_{\langle\langle i,j \rangle\rangle} \tau_z^i \tau_z^j - K' \sum_{\langle i,j \rangle} \tau_z^i \tau_z^j \quad (1)$$

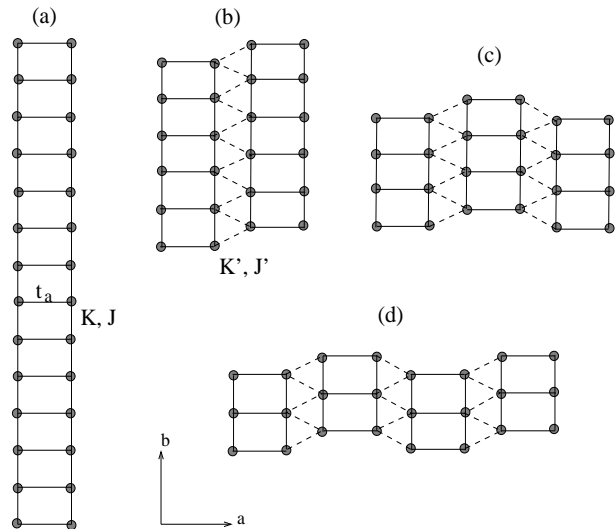


FIG. 1. Schematic representation of the crystal structure of a vanadium layer of  $\text{NaV}_2\text{O}_5$ . The vanadium ions are denoted by filled circles. The couplings in Eqs.(1 & 2) are also shown: the hopping amplitude ( $t_a$ ) on each rung, effective pseudo-spin  $K$  and spin  $J$  couplings on each ladder and between ladders  $K', J'$ . Different configurations that we have considered in exact diagonalization are denoted by: (a) A single ladder is considered with  $N = 28$ . (b) Two interacting ladders via  $K', J'$  compose a lattice of  $N = 24$ . (c) Three interacting ladders and in (d) four interacting ladders.

The first term describes the intra-rung hopping, which is the largest hopping element  $t_a$ , see Ref.( [4]). The terms  $\sim K, K'$  are effective intra- and inter-ladder Coulomb interactions, respectively [9] (Fig.1), which contain also the effect of virtual inter-rung hopping. An interesting particular case of this Hamiltonian occurs if we consider only a single ladder (i.e. set  $K' = 0$ ). Then this Hamiltonian describes the 1D Ising model in a transverse field of strength  $t_a$  whose exact solution, including the correlation functions  $\langle \tau_z^i \tau_z^j \rangle$  and  $\langle \tau_x^i \tau_x^j \rangle$  ( $j=i\pm 1$ ), is known [16]. It has been discussed in the present context in Ref.( [14]). The model is able to describe the appearance of the zig-zag charge ordering along the ladder as a function of the control parameter  $K/t_a$ ; strictly speaking an infinitesimal staggered field due to inter-ladder coupling is necessary to stabilize the order parameter [14]. Due to the peculiar structure of the Trellis lattice (rungs of neighbouring ladders are shifted by half a lattice constant

b) the inter-ladder effective Coulomb interaction  $K'$  leads to a frustration in the zig-zag CO state. If it exceeds a critical value  $K'_c$ , then the zig-zag CO is destroyed and in-line CO would be preferred. This transition corresponds to a change in the modulation vector of the pseudo-spin density  $\tau_z(\vec{Q})$  from  $\vec{Q} = (\frac{\pi}{a}, \frac{\pi}{b})$  to  $\vec{Q} = 0$ . The Hamiltonian of Eq.(1) with  $K > 0$  describes a 2D frustrated Ising model in a transverse field (ITF) on a trigonal lattice.

In this work our aim is to present a more detailed study of the correlation functions and phase diagram of this model.

It was shown in Ref. ([14]) that the spin exchange between the ladders is strongly influenced by the charge fluctuations and the charge order parameter. In this investigation the intra-rung charge fluctuations have been eliminated by using the 1D- Ising model exact solution. This is only possible for one ladder and not in the 2D frustrated Ising model appropriate for the Trellis lattice. Therefore we will keep the general interaction term of charge and spin degrees of freedom as proposed in Ref. ([9])

$$\begin{aligned}
H_{CS} = & J \sum_{\langle\langle i,j \rangle\rangle} \frac{1}{16} [(1 + \tau_z^i)(1 + \tau_z^j) \vec{\sigma}^i \vec{\sigma}^j \\
& + (1 - \tau_z^i)(1 - \tau_z^j) \vec{\sigma}^i \vec{\sigma}^j] \\
& + J' \sum_{\langle i,j \rangle} \frac{1}{32} [(1 + \tau_z^i)(1 - \tau_z^j) \vec{\sigma}^i \vec{\sigma}^j \\
& + (1 - \tau_z^i)(1 + \tau_z^j) \vec{\sigma}^i \vec{\sigma}^j] \quad (2)
\end{aligned}$$

The first and second term describe the coupling of charge fluctuations to the intra- and inter-ladder exchange, respectively. For clarity we use explicitly the R,L pseudospin projectors  $\frac{1}{2}(1 \pm \tau_z)$  in the Hamiltonian. Approximate expressions for the superexchange constants  $J, J'$  have been given in Ref. ([9]). In general we ignore superexchange paths along the ladder diagonals, although this is not completely justified [4]; we will consider its effects in a few cases. So far we have introduced a large number of coupling constants as free parameters in these models. It is not our purpose to compute the properties of them for any range of the parameters involved. Instead, we shall be interested in those values that are physically relevant for the underlying  $\text{NaV}_2\text{O}_5$  compound. They were obtained in LDA+U calculations [4] assuming full charge order. In this method, the 3d-occupation of each vanadium site is fixed and an empirical on-site Coulomb interaction  $U$  is added to the LDA potential which shifts occupied 3d-states downward and unoccupied 3d-states upward with respect to the Fermi level and in this way leads to a proper insulating state for  $\text{NaV}_2\text{O}_5$ . From these LDA+U calculations [4] the following hopping and exchange constants were obtained:  $t_a = -340$  meV,  $J = 30$  meV and  $J' = -5$  meV, i.e. there is antiferromagnetic (AF) intra-ladder and fer-

romagnetic (FM) inter-ladder exchange. As the effective inter-site Coulomb constants are not known, they are left as variable parameters in a range of up to 1 eV. The on-site Coulomb interaction, which does no longer appear in our effective low energy Hamiltonian, has the magnitude  $U = 4$  eV.

### III. LADDER HILBERT SPACE AND COMPUTATIONAL TECHNIQUE

In our numerical computation, each rung  $i$  is associated with the four dimensional Hilbert space  $\{|\sigma_i\rangle \otimes |\tau_i\rangle\}$  where  $\sigma_i, \tau_i = \uparrow, \downarrow$ . We classify the states used according to their total spin quantum number  $\sigma_z$  and restrict to the space with  $\sigma_z = 0$  for the ground state calculations. Note that the total pseudo spin z-component  $\tau_z = 0$  is not conserved due to the first term in Eq.(1). As a consequence of this, all states in the pseudo-spin sector have to be included in the calculation. Therefore the maximum number of sites which we treat is  $N=28$ . They may be arranged in different structures, some of them are shown in Fig.1. In Fig.(1-a) we have plotted an isolated single ladder where  $N=28$ . The intra-ladder coupling constant  $K$  (which is the result of Coulomb interaction on neighbouring rungs) exists on each leg of the ladder. Similarly the exchange constant  $J$  on each leg represents the coupling of the spin degrees of freedom of each electron. The hopping parameter  $t_a$  is defined on each rung. Most of our calculation on the single ladder is considered with periodic boundary condition (BC) in the legs direction. We have only considered the open BC when we compare the correlation functions of a single ladder and two coupled ladders. The interactions of two ladders is assigned in Fig.(1-b) with inter-ladder couplings  $K'$  and  $J'$  which is denoted by dashed lines. All of results presented here on two coupled ladders are in open BC. The interaction between three and four ladders is depicted in Fig.(1-c and d). The results of computations on this latter configurations are not presented here because the lattice dimension on each direction is very small and we cannot avoid boundary effects. However this results help us to see what will be the effect of more ladder interaction and find a qualitative phase diagram for our model.

We use a single ladder to study the finite size scaling of various quantities as function of the number of sites  $N$ . We also use some more two dimensional structures as shown in Fig.1 corresponding to various  $N$  to investigate the effects of inter-rung interactions, especially concerning the phase diagram as a function of  $K, K'$ . We represent correlations for open boundary conditions on the ladder since for the former the correlation functions are symmetric around the midpoint of the ladder and therefore presumably contain less information. The periodic boundary condition is applied in the b-direction and used to compute the energy levels.

## IV. RESULTS OF EXACT DIAGONALIZATION

In this section we present the results of our calculations for correlation functions of the Hamiltonian ( $H$ ) with both spin and pseudo-spin degrees of freedom ( $H = H_c + H_{CS}$ ). From this information, we are able to conjecture a phase diagram in the  $(K, K')$ - plane. Furthermore, we also study the influence of the exchange on the critical value  $K_c$  for charge ordering in the single ladder. Subsequently, we come to the important question about the nature of excited states (charge type vs. spin type) and discuss the finite size scaling of the energy gap in a single ladder. We have also considered the effect of bond-alternation (dimerization,  $\delta$ ) of the spin exchange on the single-ladder system. This shows the scaling behaviour of spin gap due to  $\gamma$ .

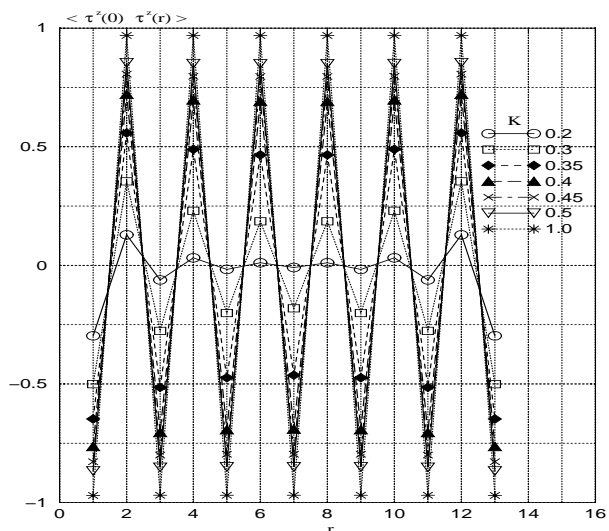


FIG. 2. Pseudospin correlation function ( $\langle \tau^z(0)\tau^z(r) \rangle$ ) for a single ladder (Fig.1-a) versus  $r$ , the distance between rungs. Periodic boundary condition are considered along legs of ladder so that the correlations are symmetric around the mid-point. By increasing  $K$ , an evolution from a disordered phase (no-long-range order) at small value of  $K$  ( $\leq 0.35$ ) to long-range order happens for large value of  $K$  ( $J=30$  meV).

### A. Correlation functions and CO transition

The pseudo-spin interaction  $K > 0$  along the ladder legs is of “antiferro” type because physically the d-electrons sitting on the same side of adjacent rungs have a larger repulsion than if they were located across the ladder diagonal. Thus the second term in Eq.(1) tends to localize the electrons on opposite sites of the ladder in zig-zag fashion (Fig.1). On the other hand the first term in Eq.(1) which describes the hopping energy within the rung prefers the disordered mixed valent state where the d-electron occupies the symmetric rung-bonding state with equal probability of sitting on the L and R sites.

This state is realized for  $K = 0$  (and  $t_a$  as given above from LDA+U calculations). If  $K$  increases above a critical value  $K_c = t_a$ , eventually the ordered state with a zig-zag correlation is preferred. This behaviour is clearly exhibited in Fig.2 for the single ladder ( $K'=0$ ).

The correlation function for a single ladder with periodic BC is plotted for  $N=28$  in Fig.(2). For small values of  $K$  ( $K < 0.4$ ) there is no LRO and correlations decay very fast. By increasing  $K$  ( $K > 0.4$ ), the correlation function shows zig-zag (alternating) LRO where the amplitude of the correlations is approximately constant for all distances ( $r$ ). The critical interaction can be seen to be  $K_c = 0.35-0.4$  eV  $\simeq t_a$ . The coupling to adjacent ladders (third term in Eq.(1)) would however prefer the “ferro” type arrangement, which leads to a frustration of charge (pseudo-spin) order. The effect of this frustration is clearly visible in Fig.3 and Fig.4 for the correlation functions with  $K' > 0$ , most directly for the  $2^{nd}$  neighbour rung ( $r=2$ ). Its correlation for  $K' = 0$  is of ferro type, then increasing  $K'$  becomes first antiferro-type and finally, when  $K'$  is large enough so that the in-line ordering is preferred, it becomes of ferro type again. This non-monotonic behaviour of  $\langle \tau^z(i)\tau^z(i+2) \rangle$  is due to the competition of different interaction paths, either directly along the legs of the given ladder, involving  $K$ , or indirectly via adjacent ladders which involves  $K'$ .

A similar behaviour is seen in the two-dimensional lattice by considering three or four ladders interacting via  $K'$ . In this case the number of rungs is reduced to four and three respectively in each ladder (Fig.1-(c) and (d)). We shall explain the case of the two-ladder system in more detail. In this case the system is composed of two 6-rung ladders with open boundary conditions imposed. The pseudo-spin correlation functions are plotted in Fig.3 and Fig.4. We have plotted  $\langle \tau^z(0)\tau^z(r) \rangle$  along the b-direction for both single and double ladder systems. The case of a single-ladder is added for comparison. In Fig.3, the value of  $K$  is fixed to  $K=0.35 < K_c$ . The case of single-ladder ( $K'=0$ ) shows a rapid decay with distance which verifies that no LRO exists in the ladder. By turning on the  $K'$  coupling, the second ladder interacts with the first one. We have plotted the correlation functions at the same points of the single-ladder for different value of  $K'$ . When  $K'=0.175$  or  $0.35$  eV, the qualitative behaviour does not change which verifies the absence of LRO. By increasing  $K'$  the ordering of the first neighbour ( $r=1$ ) goes from anti-ferro to ferro type. For the  $2^{nd}$  neighbour ( $r=2$ ) this ordering goes from ferro- to anti-ferro and finally again to ferro- type for enough high value of  $K'$  (in this case  $K' > 1.25$ ). As mentioned above, the competition between different paths of interactions via  $K$  and  $K'$  is responsible for this behaviour. It happens for  $0.35 < K' < 0.7$  eV which is a phase with no LRO and will appear in the phase diagram (Fig.5). For high value of  $K'$  an in-line LRO appears on each ladder of the model.

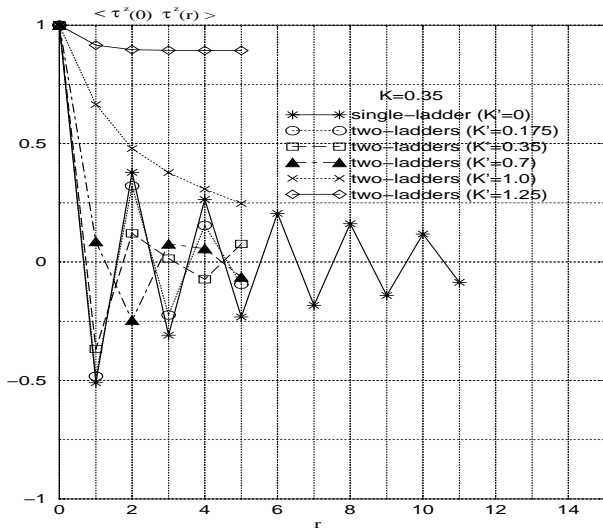


FIG. 3. Pseudospin correlation function ( $\langle \tau^z(0)\tau^z(r) \rangle$ ) for both single (Fig.(1-a)) and double ladder (Fig.(1-b)) versus distance ( $r$ ). In both cases the intra-ladder coupling ( $K$ ) is fixed to  $K=0.35 < K_c$ . Then the correlations decay very fast and do not show long-range zig-zag ordering. By increasing  $K'$  (inter-ladder coupling) deviation from single ladder results start and leads to a disorder regime for an intermediate value of  $K'=0.35$ . For sufficient size of  $K'$  an in-line ordering will appear. (Correlations computed with open boundary condition,  $J=30 \text{ meV}$  and  $J'=-5 \text{ meV}$ ).

In addition, Fig.4 shows a similar behaviour like Fig.3, while  $K$  is fixed to  $K=0.5 \text{ eV} > K_c$  in the zig-zag ordered phase of a single-ladder system. The correlation function shows that for the single-ladder ( $K'=0$ ), a true zig-zag LRO exists. As before, a small value of  $K'$  does not change the ordering of the single-ladder ( $K'=0.25$  and  $0.5 \text{ eV}$ ). For an intermediate value of  $K'$ , the disordered (no LRO) phase will appear ( $0.5 < K' < 1.5 \text{ eV}$ ). Then by increasing  $K'$  a complete in-line ordering starts to stabilise.

### B. Phase Diagram for CO

As we have seen in the previous sections, the transition from antiferromagnetic (zig-zag) to ferromagnetic (in-line) type CO depends on the ratio of  $K$  to  $t_a$  and on the “frustration” ratio  $K'/K$ . As the  $2^{nd}$  neighbour ( $r=2$ ) correlation along the ladder shows the transition is not abrupt but gradual. This signals an intermediate region in the  $K, K'$  plane which has to be considered as a phase of no LRO. We believe that this phase is very similar to the “floating phase” discovered in the 2D-ANNNI (anisotropic next nearest-neighbour Ising) model on a square lattice even though in this case it exists only at finite temperature (e.g. Ref. ([17])). The inherent geometric frustration of the Trellis lattice might stabilize it even for zero temperature. The phase diagram obtained from

systematic study of the correlation function is shown in Fig.5. For simplicity, let us neglect the spin coupling and consider Eq.(1) in two marginal cases. First, if  $K' = 0$ , Eq.(1) reduces to a one-dimensional ITF model. Then for  $K < K_c$  there is no LRO for charge degrees of freedom while a  $2^{nd}$ -order quantum phase transition will occur at  $K_c$  to an anti-ferroelectric (zig-zag) LRO. In the other extreme case where  $K=0$ , Eq.(1) is reduced to a two-dimensional ITF model on a square lattice. Obviously for small value of  $K'$ , the first term in Eq.(1) prevents the existence of LRO for charge degrees of freedom. If  $K'$  goes to large values respect to  $t_a$ , the two-dimensional square lattice shows a ferro-electric (in-line) ordering. Therefore the phase diagram of Eq.(1) in the  $K$ - $K'$  plane consists of two boundary lines which divide a phase with no LRO in the intermediate regime from the other in-line and zig-zag LRO. This phase boundary is an extension of two critical points  $K_c$  and  $K'_c$  in the  $K$ - $K'$  plane which is supported by numerical data on two-dimensional clusters (Figs.3 and 4).

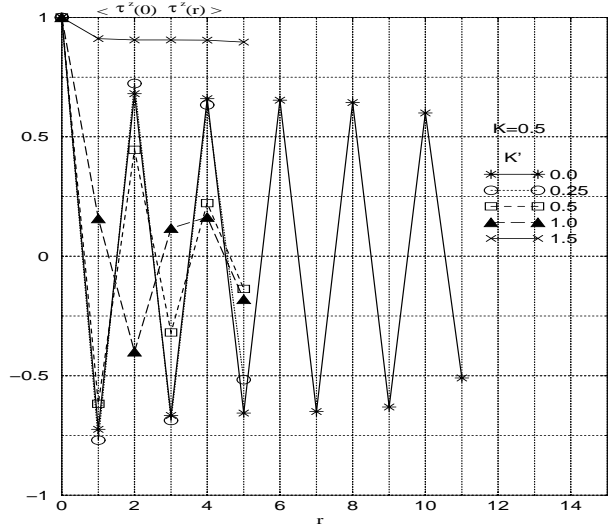


FIG. 4. This plot is similar to Fig.(3) but for different values of  $K$  and  $K'$ . Here  $K$  is fixed to  $K=0.5 > K_c$  which shows long-range zig-zag order on the single ladder ( $K'=0$ ). By turning on the inter-ladder coupling ( $K'$ ), no qualitative changes are observed for small value of  $K'=0.25$ . By increasing  $K'$ , the system goes through a disordered phase for intermediate values of  $K'=1.0$  and then enters to the in-line ordered phase for large value of  $K'=1.5$ . (Correlations are computed with open boundary condition  $J=30 \text{ meV}$  and  $J'=-5 \text{ meV}$ ).

The phase boundary for the upper in-line phase and the lower zig-zag phase are obtained by requiring a threshold value of 90% for the correlation of each type. As critical values we obtain  $K_c \simeq 0.39 \text{ eV}$  (the effect of spin coupling has been considered) and  $K'_c$  is the critical value of a two-dimensional ITF model on a square lattice including the spin coupling by Eq.(2). If we neglect the effect of Eq.(2) then  $K'_c \simeq 0.054 \text{ eV}$  [18]. These phase

boundaries enclose the disordered phase with no clearly discernible long range correlation. Although specifying the properties of the intermediate no LRO phase is beyond our numerical computations our data show that the period of oscillation of correlation functions has doubled in comparison to the zig-zag ordered phase. This can be seen in Fig.(3) at  $K'=0.7$  and in Fig.(4) at  $K'=1.0$ .

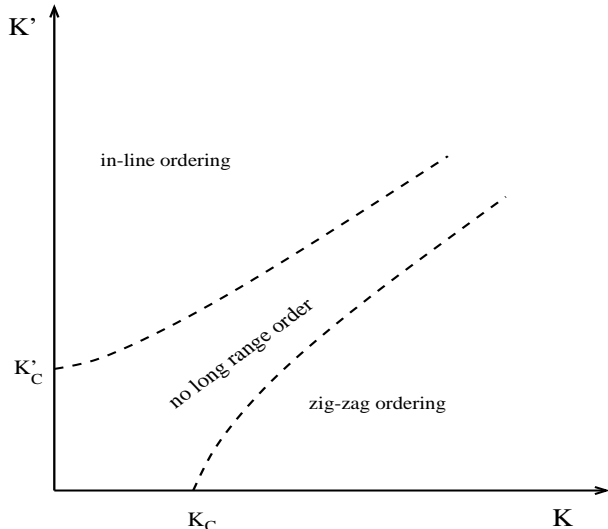


FIG. 5. Charge-order (CO) phase diagram in the space of intra-ladder ( $K$ ) and inter-ladder ( $K'$ ) couplings.  $K_c$  represent the critical value of  $K$  in a single ladder configuration (Fig.(1-a)). On the vertical axis  $K'_c$  is the critical value of a two-dimensional (ITF + spin exchange effect) on a square lattice. The dashed lines show the qualitative phase boundary between three different phases where zig-zag ordering happens in the lower-right part and in-line ordering in the upper-left. A phase with no LRO separates the two ordered phases.

The phase boundaries for CO also depend on the size of the exchange constants. This has been studied for the point  $(K, K') = (K_c, 0)$ , corresponding to the single ladder case in more detail as shown in Fig.6. The critical value  $K_c$  for development of long range order is defined by the simultaneous crossing point where curves for different ladder lengths ( $N=20-28$ ) meet. One can clearly see that  $K_c$  shifts as a function of the exchange  $J$  along the ladder leg. This can be explained as follows. In the disordered phase there is a certain amount of stabilisation energy of the spin singlet. The incipient zig-zag CO which localizes the d-electrons on opposite sites of the ladder diagonal tends to reduce this stabilisation energy and hence, if  $J$  increases the critical  $K_c$  for CO to set in also has to increase. It is shown for two different values of  $J$  (30, 100 meV) in Fig.6. In the case of single-ladder by setting  $J = 0$ , we have a one-dimensional ITF model where  $K_c = t_a$ . It is shown in Fig.6-a that the intersection of the pseudo-spin correlation function for different values of  $N$  (20, 24, 28) is at  $K_c = 0.39$  eV where  $J = 0.03$  eV ( $t_a = 0.34$  eV). A similar curve in Fig.6-b shows that

the intersection is at  $K_c = 0.40$  eV where  $J$  is increased to  $J = 0.1$  eV at fixed  $t_a$ . This verifies the monotonic dependence of  $K_c$  on the exchange constant  $J$ .

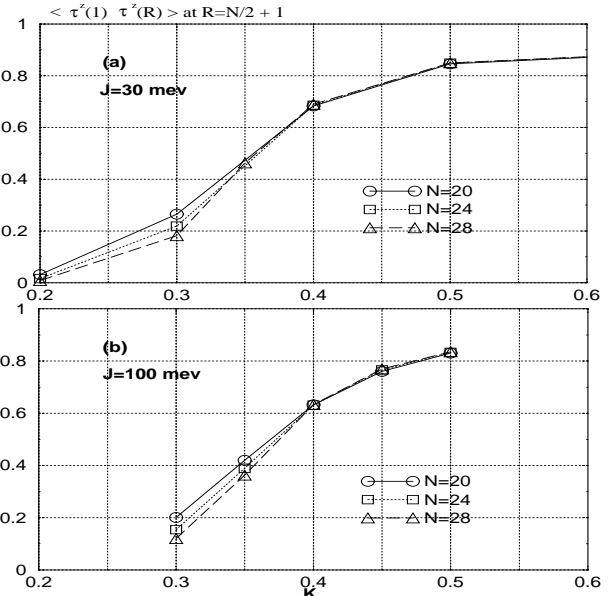


FIG. 6. The pseudo-spin correlation amplitude at fixed distance  $R = \frac{N}{2}$  versus the intra-ladder coupling ( $K$ ) for single ladder. Different sizes of ladder ( $N=20, 24, 28$ ) are implemented to track the crossing point of curves, which is the transition point. (a) The effect of spin exchange ( $J$ ) is considered with the value of  $J = 30$  meV then the crossing point happens at  $K_c \simeq 0.39$ . (b) In this case  $J = 100$  meV which causes an increase to the value of  $K_c \simeq 0.4$ . (Periodic boundary conditions are considered along the legs of ladder).

### C. Nature of excited states, finite size scaling and effective exchange

We have implemented the Lanczos method in different  $S_{tot}^z$  subspaces to determine the structure of excited states. For the single-ladder system, the ground state and first excited state are always spin singlet and triplet state respectively, as long as we do not include the exchange path along the ladder diagonals. This is true even in the coupled ladder system (2D Trellis lattice). As we have a Heisenberg exchange term, the singlet-triplet gap has to vanish in the thermodynamic limit  $N \rightarrow \infty$ .

However, from the finite size scaling behaviour we may extract the “effective exchange” along the ladder for a pure spin model, which is modified from its bare value  $J$  due to the effect of intra-rung charge fluctuations. In Fig.7-a the scaling behaviour of the singlet-triplet gap  $\Delta$  for a single ladder is shown as a function of  $1/N$  ( $N=16, 20, 24, 28$ ) for various interaction parameters  $K$ . All curves show a decrease in the energy gap with increasing  $N$ , which leads to gapless behaviour by extrapolation to  $N \rightarrow \infty$ . We use a scaling form for the energy gap

given by

$$\Delta(N) \simeq \Delta_\infty + \frac{\alpha}{N^\nu} \quad (3)$$

where  $\Delta_\infty \rightarrow 0$  for  $N \rightarrow \infty$ ,  $\alpha$  is constant and  $\nu$  a scaling exponent. These values are given in Table 1 for various  $K$  and we see that  $\nu < 1$  for  $K < K_c$  and  $\nu > 1$  for  $K > K_c$ .

$K$	$\alpha$	$\nu$
0.3	0.03379	0.75224
0.35	0.03332	0.88581
0.392	0.03633	1.04005
0.4	0.03683	1.06949
0.45	0.03699	1.21717
0.5	0.02862	1.23286

Table 1. Numerical values of the coefficients in the scaling function of the energy gap in Fig.7-a. The scaling exponent is  $\nu < 1$  for  $K < K_c \simeq 0.39$  and  $\nu > 1$  for  $K > K_c$ . The scaling form is  $\Delta = \Delta_\infty + \frac{\alpha}{N^\nu}$ . (Data has been obtained by imposing a least square root error of  $10^{-8}$  for the scaling function ).

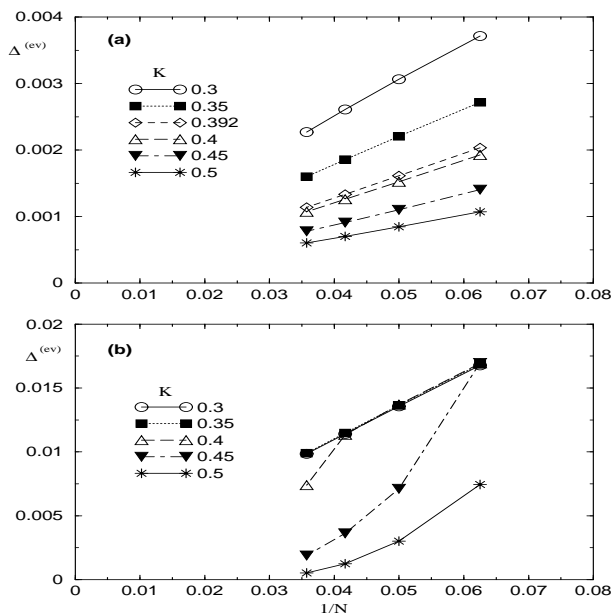


FIG. 7. The energy gap to the 1<sup>st</sup> excited state versus  $1/N$  of the single ladder (Fig.(1-a)) for different values of intra-ladder coupling ( $K$ ). (a) All data show gapless behaviour in the  $N \rightarrow \infty$ . The spin exchange is  $J=30$  meV. (b) In addition to  $J$  we have added diagonal exchange terms ( $J_d=32.7$  meV) on each plaquette of ladder. For  $K < K_c=0.39$ , we observe qualitative behaviour similar to part (a) where the first excitation is a spin triplet. But for  $K > K_c$  the behaviour is completely different because the excitations are charge type. The excited state has the same total spin  $S_{tot}=0$ .

This shows the different curvature of  $\Delta$  versus  $1/N$ . (To have the best fit of the data in Fig.7-a at fixed  $\nu = 1$

we have considered more terms in the curve fitting form;  $\Delta(N) = \Delta_\infty + \frac{C_1}{N} + \frac{C_3}{N^3} + \frac{C_5}{N^5}$  which is justified for the case of pure spin- $\frac{1}{2}$  chain [19]). For a pure spin- $\frac{1}{2}$  system without coupling to charge degrees of freedom, one has  $\nu=1$  and the coefficient  $C_1$  is related to

$$C_1 = 2\pi^2 S^2 J_{\text{eff}} \quad (4)$$

Comparison with our  $C_1$  coefficient from the scaling plots in Fig.7-a gives us the variation of the effective exchange constant  $J_{\text{eff}}(K)$  with the interaction  $K$  that controls the charge order (for a given  $t_a$ ). This variation is shown in Fig.8. A steep drop in  $J_{\text{eff}}(K)$  is seen in the region where the charge order sets in ( $K \simeq 0.39$ ). Eventually for  $K \gg t_a$  when zig-zag CO is almost complete,  $J_{\text{eff}}$  has to approach zero because in the zig-zag structure the exchange  $J$  along the legs is ineffective.

The situation changes when we also include exchange along the ladder diagonals. In this case we will add an exchange term similar to the first term of Eq.(2) along the ladder diagonal in each plaquette (not shown in Fig.1). The value of diagonal exchange is considered to be  $J_d = 32.7$  meV which has been obtained by LDA+U calculations in Ref.([4]). For  $K < K_c$  the first excited state is a spin triplet, for  $K > K_c$  however the first excited state is not a spin triplet, rather it has spin zero like the ground state and therefore it should be interpreted as a charge excitation. This leads to a very different scaling of the energy gap for  $K > K_c$  (Fig.7-b) while the case  $K < K_c$  is very similar to the model without diagonal exchange (Fig.7-a). The scaling behaviour in Fig.7-b for  $K < 0.35$  is roughly linear which behaves like the former spin excitations while for  $K > 0.4$  the scaling behaviour is completely different.

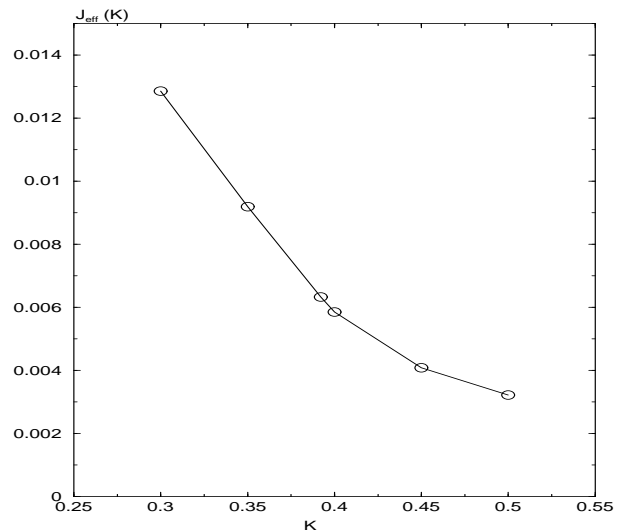


FIG. 8. Effective superexchange coupling versus  $K$ . It shows a steep decrease close to the transition point  $K_c=0.39$ . Moreover the effective exchange goes to zero in the completely zig-zag ordered phase ( $K \rightarrow \infty$ ).

We have also considered the effect of dimerization ( $\delta$ ) of the exchange coupling on the energy gap of a single-ladder. This is of interest because it seems now clear that the charge disordered ladders in the low temperature structure of  $\text{NaV}_2\text{O}_5$  discussed in the introduction have a large superexchange dimerisation due to the shift of oxygen positions [4]. Therefore we consider the influence of the dimerisation for  $K < K_c$  in the disordered regime. This means that the exchange constant ( $J$ ) of the first term in Eq.(2) is replaced by  $J(1 \pm \gamma)$  in an alternating way. The dimerization parameter varies as  $\gamma = 0.01, 0.05, 0.1, 0.2, \dots, 0.6$ . Obviously an energy gap opens by turning on  $\gamma$  which does not scale to zero with increasing  $N$  ( $N \rightarrow \infty$ ) as it did for the undimerized case  $\gamma = 0$ . In Fig.9-b we have plotted the log-log plot of energy gap versus  $\gamma$ . For small value of  $\gamma$  the energy gap scales as  $\Delta \sim \delta^\eta$  where  $\eta = 2.25 \pm 0.25$ .

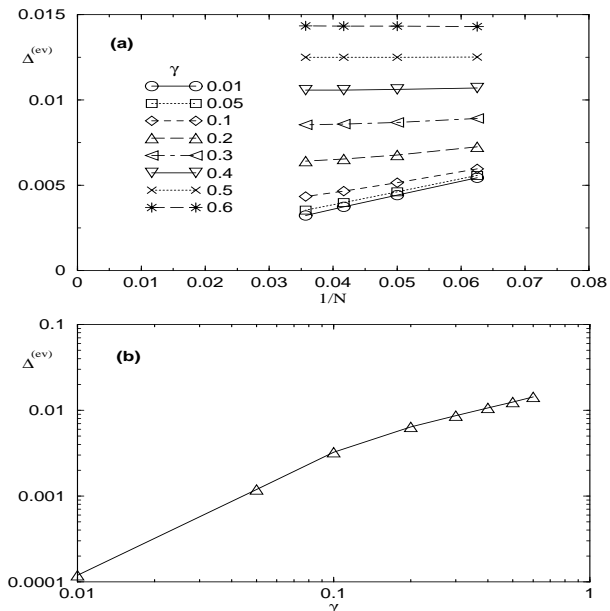


FIG. 9. Spin gap energy versus  $1/N$  in the dimerized single-ladder for  $K=0.2 < K_c$  and  $J=30 \text{ meV}$ . (a) Data are plotted for different value of dimerization parameter ( $\gamma = 0.01, \dots, 0.6$ ). All curves show up a finite gap in the  $N \rightarrow \infty$  (for  $\gamma > 0.05$  it is more apparent). (b) The extrapolated energy gap is plotted versus  $r$  in a log-log scale. For small value of  $\gamma$  ( $\gamma < 0.1$ ) we observe the scaling behaviour,  $\Delta = \gamma^\eta$ .

## V. SUMMARY

The main results of our exact diagonalisation investigation for the present  $\text{NaV}_2\text{O}_5$  model are the following: For the single ladder the ratio of  $K/t_a$  controls the onset of charge order which is observed in the evolution of the pseudospin correlation function (Fig.2). This is similar as in the exact 1D Ising model in transverse field results [16].

For the 2D Trellis lattice, it depends on the relative size of intra- and inter-ladder effective Coulomb interactions  $K, K'$  and the size of  $K$  with respect to the intra-rung hopping  $t_a$  whether in-line or zig zag structures are realized. This agrees with LDA+U total energy calculations which show that these two structures are very close in energy with the zig-zag structure slightly lower [4]. In addition however we have shown that in a wide region in the  $K, K'$  plane a disordered phase should exist which does not show long range correlations of charge due to the inherent frustration of the Trellis lattice structure. According to Lüdecke et al [8] in the real  $\text{NaV}_2\text{O}_5$  structure only every second ladder is charge ordered and the intervening ladders stay in the MV state. This might be an indication that  $\text{NaV}_2\text{O}_5$  is not far from the regime with a disordered state, i.e. close to a quantum critical point. We have also studied the effect of spin coupling on the charge order transition. We have shown that  $K_c$  has a monotonic dependence on the exchange constant ( $J$ ), i.e. for  $J=30 \text{ meV}$  it leads to 15 percent increase of the 1D ITF result.

We have addressed the issue of excitation type in our charge-spin model. As long as the spin exchange along the ladder diagonal is absent the excitations are singlet to triplet. By adding a diagonal spin exchange on ladders we will observe charge excitations in the ordered phase while it is still spin type in the disordered phase.

From the finite size scaling analysis of the singlet triplet excitation gap we obtain the dependence of the effective inter-rung exchange on the ladder as function of the degree of charge order, i.e. as function of  $K$ . A steep drop of  $J_{eff}$  is observed around the critical value  $K_c$  for charge order. Eventually it will be reduced to zero in the fully CO regime in qualitative agreement with perturbation calculations [14]

## VI. ACKNOWLEDGEMENT

A.L. would like to thank A. Bernert, V. Yushankhai and I. Peschel for fruitful discussions and acknowledge Max-Planck-Institute for the Physics of Complex Systems for computer facilities and M.A.M.D. would like to thank the Centro de Supercomputación Complutense for the allocation of CPU time in the SG-Origin 2000 Parallel Computer. M.A.M.-D. was supported by the DGES spanish grant PB97-1190.

[1] Y. Fuji, et.al J. Phys. Soc. Jpn. **66**, 326 (1997).

[2] S. Ravy, J. Jegoudez and A. Revcolevschi, Phys. Rev. B **59**, R681 (1999).



- [3] H. Smolinski, C. Gros, W. Weber, U. Peuchert, G. Roth, M. Weiden and C. Geibel, Phys. Rev. Lett. **80**, 5164 (1998).
- [4] A.N. Yaresko, V.N. Antonov, H. Eschrig, P. Thalmeier and P. Fulde, Phys. Rev. B **62** (2000).
- [5] P. Horsch and F. Mack, Eur. Phys. J. B **5**, 367 (1998).
- [6] M. Isobe and Y. Ueda, J. Phys. Soc. Jpn. **65**, 1178 (1996).
- [7] T. Ohama, H. Yasuoka, M. Isobe and Y. Ueda, Phys. Rev. B **59**, 3299 (1999).
- [8] J. Lüdecke, A. Jobst, S. van Smaalen, E. Morre, C. Geibel and H.-G. Krane, Phys. Rev. Lett. **82**, 3633 (1999).
- [9] P. Thalmeier and P. Fulde, Europhys. Lett., **44**, 242 (1998).
- [10] L.P. Regnault, J.E. Lorenzo, J.-P. Boucher, B. Grenier, A. Hiess, T. Chatterji, J. Jegoudez, A. Revcolevschi, Physica B **276-278**, 626 (2000).
- [11] P. Thalmeier and A. N. Yaresko, Eur. Phys. J. B **14** 495, (2000).
- [12] H. Nakao, et.al Phys. Rev. Lett. **85**, 4349 (2000).
- [13] A. Bernert, T. Chatterji, P. Thalmeier and P. Fulde, *preprint*
- [14] V. Yushankhai and P. Thalmeier, cond-mat(0008322).
- [15] J. L. de Boer, et.al preprint cond-mat(0008054).
- [16] P. Pfeuty, Ann. Phys. (N.Y.) **57**, 79 (1970).
- [17] P. Bak, Rep. Prog. Phys. **45**, 587 (1982).
- [18] P. Pfeuty and R. J. Elliott, J. Phys. **C: Solid St. Phys.** **4**, 2370 (1971).
- [19] A. Auerbach in *Interacting Electrons and Quantum Magnetism* (Springer-Verlag, New York 1994).